


Cite this: *RSC Adv.*, 2021, **11**, 35274

# Realization of multi-configurable logic gate behaviour on fluorescence switching signalling of naphthalene diimide congeners†

Hridoy Jyoti Bora,<sup>a</sup> Pranjal Barman,<sup>b</sup> Sushanta Bordoloi,<sup>c</sup> Gautomi Gogoi,<sup>a</sup> Bedanta Gogoi,<sup>d</sup> Neelotpal Sen Sarma<sup>b</sup> and Anamika Kalita<sup>b\*</sup>

Organic entities like suitably functionalized naphthalene diimide (NDI) exhibited logical behaviours in response to various external stimuli and can be used to develop digital logic operations. The present findings include utilization of two congeners of NDI *i.e.*, N1 and N2 for the successive turning ON/OFF of fluorescence with inclusion of acid and base. The recognition of the switching phenomenon of the probes N1 and N2 are applied to construct fundamental digital logic gates such as NOT, YES, IMPLICATION, INHIBIT, *etc.* The inputs to each of the logic gates are defined by the presence or absence of acid and base. Accordingly, the outputs generated from the gates are in the form of fluorescence ON or OFF status denoted by "1" and "0" respectively. Likewise, we have adopted Boolean algebra and its associated De-Morgan's theorem to build the combined logic gates such as XOR and XNOR gates. The proposed logic gates are validated by the optical behaviour of the congeners N1 and N2 in response to acid as well as base and the experimental results are confirmed by the theoretical predictions. The proposed work can have potential applications in next-generation logic based analytical applications.

Received 7th September 2021  
Accepted 17th October 2021

DOI: 10.1039/d1ra06728a

rsc.li/rsc-advances

## Introduction

In recent years, investigation of new organic materials magnetized the attention of the scientific community owing to their outstanding properties. Switching and fine-tuning of optical properties of organic molecules is of immense interest both in the field of fundamental research as well as for real-time applications such as security inks, sensors, display and memory devices, logic gates, *etc.*<sup>1–5</sup> The conformation of fluorophore groups, packing and interactions play an important role in optical properties. Various strategies are applied to tweak the molecular switching properties such as chemical modification, polymorphism, and nanofabrication. Among which tailored chemical design *via* organic synthesis is the most scrutinized technique to tune the organic fluorescence,<sup>6</sup> which includes the alteration of the molecular packing or the HOMO–

LUMO energy level that often-produced supramolecular building blocks. Generally, molecular switches respond to various external stimuli, such as physical stimuli like light, voltage, mechanical stress, magnetic field, *etc.* and chemical stimuli such as pH, chemical reagent, *etc.*<sup>7–13</sup>

Supramolecular self-assembly emerges as an effectual aid to produce luminescent materials, as the photophysical characteristics can be homogenized by the reversible non-covalent interactions of the systems. Distinguished from traditional chemistry which was erected by covalent interactions, supramolecular chemistry gives prominence on reversible and non-covalent interactions encompassing  $\pi$ – $\pi$  interactions, hydrogen bonding, electrostatic effects, host guest interactions, *etc.*<sup>14</sup> Supramolecular self-assembly of  $\pi$ -conjugated chromophores<sup>15–17</sup> mediated by hydrogen bonding<sup>18</sup> yields an electrifying opportunity to exploit the multidirectional nature of the classic non-covalent interaction, which are the emerging class of materials that have applications in wide range of fields.<sup>19</sup> This explicitly defines the structural framework of photo-physically abundant building blocks in the self-assembled state, which often leads to hierarchical arrangements with divergent luminescent properties<sup>20</sup> and transport properties,<sup>21,22</sup> especially if the building blocks are semiconductor in nature. Among diverse functional materials, derivatives of naphthalene diimide (NDI) are the potential candidates owing to varied tunable properties.<sup>23</sup> Even though NDI shows very weak emissions, however, changing the substituents significantly affect the

<sup>a</sup>Physical Sciences Division, Institute of Advanced Study in Science and Technology, Paschim Boraigaon, Guwahati-781035, Assam, India. E-mail: anamik.kalita01@gmail.com

<sup>b</sup>Department of Electronics and Communication Technology, Gauhati University, Guwahati-781014, Assam, India

<sup>c</sup>Department of Electronics and Communication Engineering, National Institute of Technology Mizoram, Aizawl-796012, India

<sup>d</sup>Department of Chemistry, Gauhati University, Guwahati-781014, Assam, India

† Electronic supplementary information (ESI) available: Synthetic scheme of N2, <sup>1</sup>H-NMR, ESI-MS, FT-IR spectra, NOT and YES logic gate and truth tables. See DOI: 10.1039/d1ra06728a



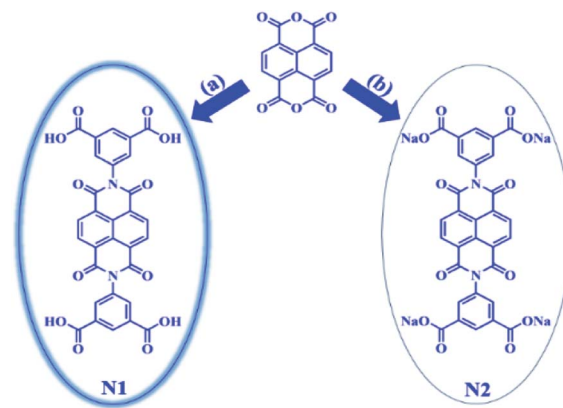
optical properties of NDI.<sup>24,25</sup> Efforts have been made to increase the fluorescence and self-organization properties by core substitution with amino groups<sup>26</sup> and N-substitution with highly directional H-bonding interactions *via* chemical modifications.<sup>27,28</sup>

Modern day research provides the opportunity to work in the multidisciplinary subjects sharing a common platform to exchange new ideas, creating new innovations to develop smart and efficient products. In that context, molecular level logic function has become one of the emerging research topics in chemical sciences for miniaturization of technology and intelligent products. In the digital electronics, the logical functions can be realized in terms of Boolean algebra that was discovered by George Boole in 1847.<sup>29</sup> Likewise, the molecular logic gates<sup>30,31</sup> also fulfil Boolean algebra by acquiring chemical, optical or biological inputs and accordingly produce a single output.<sup>32,33</sup> This offers a new paradigm shift for future computing technology that facilitates with increasing functionality, reducing in size and cutting in cost. In recent decades, many biological and chemical systems have displayed the feasibility to effectuate various Boolean logic operations such as AND, YES, NOT, OR, NAND, IMPLICATION (IMPLY), INHIBIT (INHIB), XOR, XNOR, *etc.* The fluorescent response from a photonic logic gate under the influence of specific external stimuli as inputs can be interpreted as logical output for the respective gate. Considering the reports available on molecular level logic gates based on NDI moieties have witnessed the emergence of the aforesaid topic for development of next generation molecular scale electronic devices.<sup>34</sup> Ajayakumar *et al.*, have established the use of tetra-stable naphthalene diimide and realized a set of combinational logic gates (AND, half-adder) applying multichannel signal read-outs of the thermal electron transfer (ET) and intramolecular charge transfer (ICT) based reactions.<sup>35</sup> In this context, Selvan *et al.*, demonstrated a naphthalene diamine-based  $\beta$ -diketone derivative for ON/OFF fluorescent chemo-sensor for selective detection of divalent iron and copper ions and established the OR and XOR logic gate behaviour for their system.<sup>36</sup> Similarly, Singharoy *et al.*, and Yang *et al.*, with the help of naphthalimide as precursor, have demonstrated the combinational logic gate behaviour along with their different applications.<sup>37,38</sup>

In view of the competitive advantages mentioned above, we have demonstrated a fluorescence switching phenomenon of NDI probes in response to the external stimuli and realized their behaviour in binary format to implement in digital logic gates. The novelty of the presented work lies in achieving the modulation of fluorescent ON/OFF switching using NDI congeners concerning the use of external stimuli. Accordingly, we have demonstrated these behaviours in the form of logic gate operations. The experimental results evinced the predictions that we have derived from the Boolean algebra.

## Results and discussion

The synthetic route of both the congeners of NDI *i.e.*, N1 and N2, isophthalic acid functionalized naphthalene diimide ligand follows a simple condensation reaction (Scheme 1). The



**Scheme 1** Synthetic scheme of N1 and N2 with synthesis condition (a) 5-amino isophthalic acid in DMF, 100 °C, overnight and (b) Na-salt of 5-amino isophthalic acid in water, overnight, respectively.

formation of N1 is established by employing the standard characterization techniques such as <sup>1</sup>H-NMR, ESI-MS, *etc.* which was already reported in our previous work<sup>39</sup> and utilized in this investigation as it is. The formation of N2 involves two steps, firstly, to prepare the sodium salt of 5-amino isophthalic acid followed by a simple condensation reaction. The detailed synthetic scheme of N2 and characterization spectra are presented in Scheme S1 and Fig. S1–S3, ESI.†

Derivatives of NDI are the crucial compounds that fascinated the scientific community due to its key features in a wide range of applications. The most beneficial part about NDI's is that one can easily tune its properties by changing the substituents.<sup>23</sup> NDI functionalized through core or diimide nitrogen shows variable photophysical properties. The synthesized congeners N1 and N2 exhibits characteristic absorption bands in solution phase at  $\lambda_{\text{max}}$  380 nm, 362 nm and 340 nm respectively as shown in Fig. S4, ESI.† While concerning the fluorescence characteristics of both the synthesized compounds, it was found that N1 is emissive under UV lamp, 365 nm, with fluorescence quantum yield of 5.1% (0.051), while N2 is non-emissive in nature (Fig. 1). To investigate their molecular switching behaviour towards external stimuli/agents, emission response experiments were carried out for both the congeners N1 and N2 respectively.

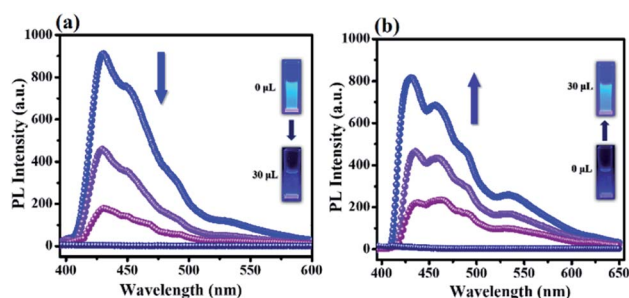


**Fig. 1** (a) Emission spectra of N1 with gradual addition of 1 mM NaOH solution, (b) emission spectra of N2 with gradual addition of 1 mM HCl solution, insets are the corresponding change in fluorescence color under UV light, 365 nm.

Emission spectra were recorded for both the congeners in aqueous medium towards the addition of external stimuli such as acid (HCl) and base (NaOH). By adding up to a 30  $\mu\text{L}$  of base to N1 system in aqueous medium ( $\text{pH} = 6$ ), the emission intensity of N1 completely diminished, reaching its minimum as shown in Fig. 1a. Further addition of extra NaOH solution does not have any noticeable effect on the fluorescence intensity. The change of color from fluorescent to non-fluorescent upon addition of base, under UV lamp, 365 nm is shown in inset of Fig. 1a. Similarly, for the non-fluorescent N2 system it was found that upon gradual increase in the amount of acid, the emission intensity of N2 increases, reaching its maximum upon addition of 30  $\mu\text{L}$  of HCl ( $\text{pH} = 5$ ) as shown in Fig. 1b. Addition of extra HCl solution does not have any significant effect on the fluorescence intensity. The change of color from non-fluorescent to fluorescent upon addition of acid, under UV lamp, 365 nm is shown in inset of Fig. 1b.

Various reasons encompass the fluorescence enhancing behaviour of NDI moieties which includes  $\pi$ - $\pi$  interactions, hydrogen bonding, electrostatic effects, host guest interactions, *etc.*<sup>14</sup> Supramolecular self-assembly of  $\pi$ -conjugated chromophores mediated by hydrogen bonding yields an electrifying opportunity to exploit the multidirectional nature of the classic non-covalent interaction.<sup>19</sup>

NDI functionalized through diimide nitrogen having highly directional and finite H-bonding interaction sites may generate supramolecular structures holding intriguing luminescence properties.<sup>40</sup> To validate the assumption, molecular simulations have been performed by DFT for a better understanding of the insight molecular interactions which governs their photo-physical properties and presented in Fig. 2. The H-bonding mediated tuning of the fluorescence property is quite unusual and rare,<sup>41–43</sup> but proximity effects<sup>44,45</sup> were employed to demonstrate the intensity enhancement by intermolecular H-bonding. Intermolecular H-bonding enlarges the energy gap between  $\pi$ - $\pi^*$  and  $n$ - $\pi^*$  which parallelly enhances the fluorescence intensity.<sup>41,46</sup> While performing the DFT calculations on the dimer models, for N1 system, the  $-\text{C}=\text{O}$  group of anhydrides of one moiety forms intermolecular H-bonding (2.35 Å) with the  $-\text{OH}$  group of acid of another moiety

(Fig. 2a), which may be the reason for subsequent increase in the fluorescence intensity. Whereas, in case of N2 dimer model, calculations revealed the lack of such intermolecular interactions with neighbouring moieties that results in non-fluorescence nature of N2 (Fig. 2b).

To get insight into the bonding interactions involved in the studied compounds, non-covalent interaction (NCI) analysis is performed using Multiwfn software. Isovalue for the visualization of the interaction is set at 0.5. The color bar indicates the type of bond formed within the compound. Blue and green color is significance of attractive bonding (H-bonding and van der Waals bonding), and red color denotes repulsive bonding. A prominent green color map appears between O22 of one monomer with H116 of other monomer of N1 compound (Fig. 3), but this contour plot is negligible in the case of N2 dimer (Fig. S5, ESI†), which supports H-bonding in the former case as well.

To further support the intermolecular H-bonding interaction, FT-IR analysis on both the congeners were carried out and presented in Fig. S6, ESI.† Comparing the FT-IR spectra of N1 with N2, due to the presence of H-bonding in N1 moiety, the  $-\text{C}=\text{O}$  peaks of acid shifted from  $1712\text{ cm}^{-1}$  to  $1706\text{ cm}^{-1}$  and  $-\text{C}=\text{O}$  peaks of amide shifted from  $1676\text{ cm}^{-1}$  to  $1670\text{ cm}^{-1}$ , with simultaneous broadening of the peaks in N1 as compared to N2 system. In the same way, the broad peak ranges from  $2500\text{ cm}^{-1}$  to  $3400\text{ cm}^{-1}$  attributed by the overlapping band of O-H and C-H stretching, which was absent in case of N2.<sup>47,48</sup> This complete investigate highlight that the noncovalent H-bonding interaction may be significant for tunable optical properties of the probes.

### Logic gate construction

Instigated by the acid-base responsive tunable optical properties, we employed our designed NDI congeners, N1 and N2 to construct fluorescent molecular logic gates capable of designing several logic operations. The logic gate operation is generally used to make a firm decision based on multiple true or false events. In this work, multiple logic systems can be formulated by rationally defining logic states based on acid-base mediated signal response. In the proposed work, the aqueous solutions N1 and N2 served as platforms for the logic operation, and the

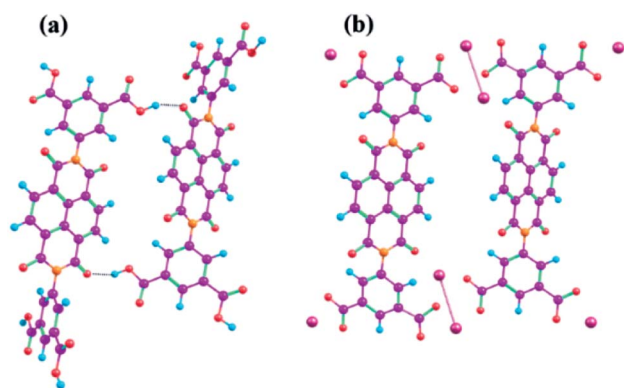


Fig. 2 Optimized geometry of N1 and N2 dimer model (a) showing H-bonding, and (b) absence of H-bonding, respectively, generated in ChemCraft software.

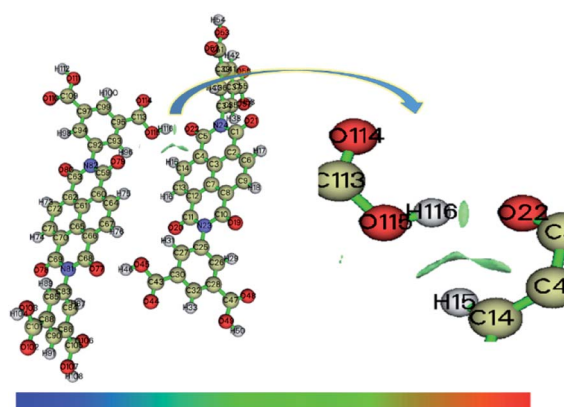


Fig. 3 Noncovalent interaction in N1 system.





external stimuli like acid (HCl) and base (NaOH) were used as logic inputs. Consequently, the generated spectral changes after the aforementioned reactions served as logic outputs. The outputs are essentially following the most renowned Boolean algebra which is vital for any digital computations. Therefore, the changes can be interpreted in terms of digital logic to develop molecular level digital devices. In the digital domain, the presence and absence of inputs are defined as logic “ON” or “1” and logic “OFF” or “0” respectively. In this work, we have represented various states of the output signal in terms of “1” and “0” and accordingly developed the truth tables associated with each logic gates. The fluorescence of N1 can be selectively quenched by base as shown in Fig. 1a. This can be ascribed due to the formation of sodium salt of carboxylic acid functionalized NDI congener upon addition of NaOH to N1 system which is further confirmed by ESI-MS Data (Fig. S7, ESI†). Similarly, for the N2 system, which is non-fluorescent in nature, revived back its fluorescence in response to the acid as shown in Fig. 1b. Upon addition of HCl to N2 system confirmed formation of isophthalic acid functionalized NDI congener as supported by ESI-MS Data (Fig. S8, ESI†). This convertible nature induced fluorescence switching of both the congeners has been used for digital logic construction in this present work. To construct molecular level logic gates, the input state can be either “0” or “1” based on the absence and presence of input. Accordingly, the output is “0” corresponding to the fluorescence “OFF” emission intensity and “1” corresponding to the fluorescence “ON” emission intensity. We perceived that in presence of base (*i.e.*, input = 1), the fluorescence of N1 was quenched (*i.e.*, output = 0). This behaviour serves the requirements of a digital NOT gate operation in which the output logic is completely opposite to that of the input logic (Fig. S9, ESI†).<sup>49</sup>

On the other hand, the addition of acid to the non-fluorescent probe N2 (*i.e.*, input = 1) can revived the fluorescence of the system (*i.e.*, output = 1). This behaviour could be utilized to develop a “YES” logic gate (Fig. S10, ESI†).<sup>44</sup> The “YES” logic can also be termed as a buffer logic in digital electronics that has several vital roles in digital computations. With the help of the aforementioned logic level derivations, we can demonstrate a new logic gate that is known as IMPLICATION (IMPLY) logic gate<sup>46</sup> for the system N1. The IMPLY gate is a behavioural gate in which an inherent NOT logic gate is present at the input side of the gate as depicted in Fig. 4. The behaviour of the IMPLY gate shows that, the output remains highly fluorescent (*i.e.*, output = 1) when both the inputs are absent (*i.e.*, inputs = 00). The presence of only NaOH input (*i.e.*, input = 10) leads to quenching of fluorescence (output = 0).

In the other case, when only HCl is present (input = 01), the fluorescence has been recovered (output = 1). Finally, the presence of equimolar amounts of both the inputs NaOH and HCl (input = 11), the fluorescence output remains high (output = 1). The experimental outcomes appropriately describe the behaviour of the proposed IMPLY gate as illustrated in Fig. 4.

Now, with the help of N2 system, we can derive the second logic gate which can be termed as INHIBIT (INHIB)<sup>50</sup> logic gate. In the INHIB gate, the absence of both inputs (input = 00), results in no change in the emission intensity (output = 0) for

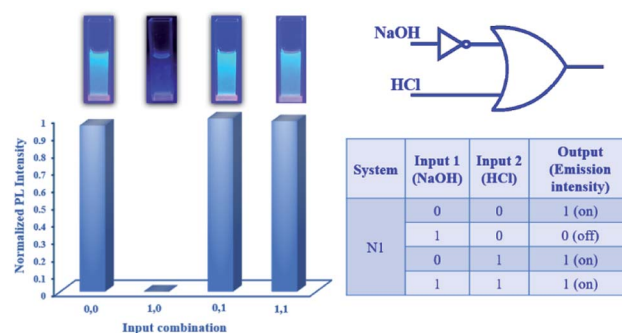


Fig. 4 IMPLY logic gate representation and corresponding truth table obtained for N1 system.

N2 system. The presence of only NaOH input (*i.e.*, input = 10) fails to recover the fluorescence (output = 0). However, in presence of only HCl (input = 01), the system recovers the fluorescence (output = 1). Finally, in presence of both the inputs *i.e.*, HCl and NaOH in equimolar amounts (input = 11), the system fails to recover the fluorescence (output = 0) (Fig. 5).

The developed logic systems based on acid–base responsive N1 and N2 congeners, we can achieve very high sensitivity and faster response that carries potential applications in decision making operations such as digital computation, control mechanism *etc.*

In order to diversify the applications of the proposed logic gates, we have explored the basic algebra associated with the digital logic operations, commonly known as Boolean algebra. With the help of this algebra, we can formulate some other complex logic gates. To derive some of the more complex gate formulations, we have used the well-known De Morgan's theorem which can convert any product of the logic inputs into the summation of the respective inputs. Furthermore, we can develop a new Boolean expression for EX-OR or XOR (exclusive OR) gate. While considering the XOR gate operation, in which the output will be logic “1” only when both the inputs are in different logic levels. Conversely, the output of the XOR gate is “0” when both the inputs are in same logic levels. The digital circuit formulation using IMPLY and INHIB gate is shown in Fig. 6a along with the respective truth table and symbol.

Similar to the XOR gate, we can derive the expression for EX-NOR or XNOR gate in terms of IMPLY and INHIB gates. It is

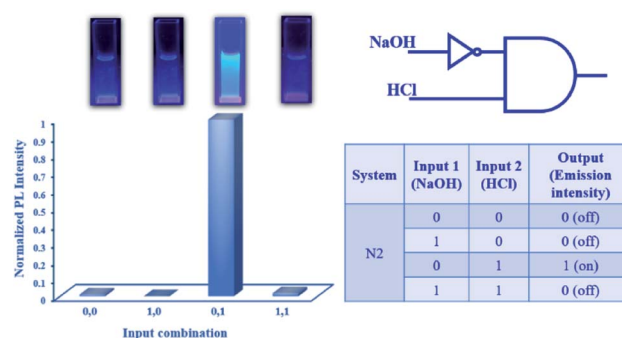


Fig. 5 INHIB logic gate representation and corresponding truth table obtained for N2 system.



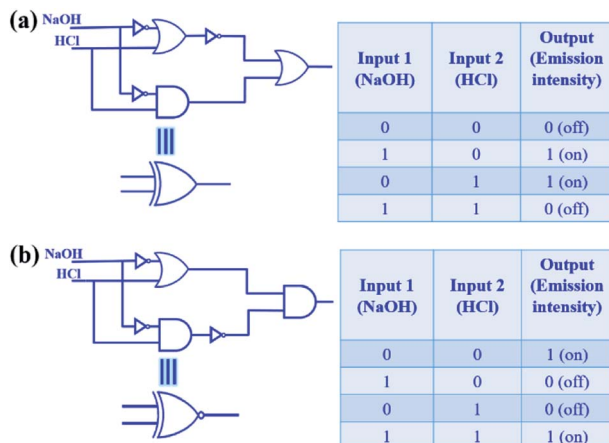


Fig. 6 (a) XOR logic gate, (b) XNOR logic gate, and corresponding truth table.

worth mentioning that the XNOR gate behaves completely opposite to that of the XOR gate. The XNOR gate formulations using both IMPLY and INHIB gate is illustrated in Fig. 6b along with the truth table and the symbol.

## Conclusions

In summary, we would like to emphasize that, the concept of molecular logic gate is already remarkable, but the coming era of information processing molecular devices based on small molecules will have a transformative impact on modern science and technology. By taking into account, the current findings described fluorescence “ON/OFF” switching signalling phenomenon based on NDI congeners in response to stimuli *i.e.*, acid and base. The corresponding multi-configurable logic gate operations such as YES, NOT, INHIBIT (INHIB), IMPLICATION (IMPLY), XOR, and XNOR *etc.* were successfully implemented for the aforesaid NDI congeners. Altogether, this investigation adds a new dimension to the design of NDI congeners along with the implementation of logic gates for future technological advancement.

## Experimental section

### Materials and characterizations

1,4,5,8-Naphthalenetetracarboxylic dianhydride (NTCDA) (Sigma-Aldrich), 5-aminoisophthalic acid (SRL), DMF (Sigma-Aldrich), NaOH (SRL), and HCl (35% Merck) used without further purification. All additional reagents used were of analytical grade. The  $^1\text{H-NMR}$  spectra were recorded on a Bruker Ascend 600 MHz Spectrometer. Mass spectrometric data Shimadzu UV-Vis spectrophotometer, UV-2600 is used to record the absorption spectra were gained from a THERMO 3000 Exactive Plus Orbitrap Mass Spectrometer. Fluorescence spectra data were recorded on a FP-8300 JASCO Spectrofluorometer, DFT calculations were performed on Gaussian 09 software using B3LYP/6-31G(d,p) level of theory and the visualization is done in ChemCraft software. Non-covalent

interaction (NCI) analysis were performed on Multiwfn software using the optimized files generated in Gaussian 09 software. Fourier-transform infrared spectroscopy (FT-IR) were carried out on PerkinElmer Spectrum-Two over the range of 4000 to 400  $\text{cm}^{-1}$ . Photographs were taken on a Nikon Coolpix digital camera.

### Synthesis of isophthalic acid functionalized NDI ligand (N1)

N1 was used directly for the above-mentioned investigation from the stored product which was synthesized earlier following the previously reported procedure.<sup>39</sup>

### Synthesis of sodium salt of isophthalic acid functionalized NDI ligand (N2)

N2 was synthesized according to the previous reported process.<sup>51</sup> At first,  $-\text{COOH}$  group of 5-amino-isophthalic acid was neutralized by a stoichiometric amount (2 equivalent) of aqueous NaOH solution to obtain sodium 5-amino-isophthalate.<sup>52</sup> Then the prepared sodium 5-amino-isophthalate (230 mg, 1.5 mmol) was added to 8 mL of distilled water in a 25 mL round-bottom flask and subjected to continuous stirring. 1,4,5,8-Naphthalenetetracarboxylic dianhydride (NTCDA) (200 mg, 0.75 mmol) was added to the solution, at a temperature of 0  $^{\circ}\text{C}$ . The solution was left stirring, while reaching the reaction mixture to room temperature. After overnight stirring, the mixture was filtered and washed with water several times to obtain the solid product. Yield: (0.36 g, 73%);  $^1\text{H-NMR}$  (600 MHz,  $\text{D}_2\text{O}$ ,  $\delta_{\text{ppm}}$ ): 8.71 (s, 4H), 7.89 (s, 2H), 7.66 (s, 4H); FT-IR ( $\text{cm}^{-1}$ ): 3430, 2924, 1712, 1676, 1450, 1348, 1248, 1156, 904, 770; ESI-MS:  $m/z$  for  $\text{C}_{30}\text{H}_{10}\text{N}_2\text{O}_{12}\text{Na}_4 (\text{M} - \text{H})^-$  calcd.: 680.982, found 680.441.

### Preparation of stock solution

Solutions of all the compounds, *viz.* N1, N2, HCl and NaOH, at a concentration of 1 mM were prepared in water for the investigation.

### Quantum yield measurement

For the compound N1, the quantum yield ( $\Phi$ ) was calculated using a standard reference dye, quinine sulfate, by employing a standard procedure.<sup>53</sup> For the calculation of fluorescence quantum yield, different concentrations of N1 were made, all of which had absorbance less than 0.1 nm at 365 nm. The literature value of  $\Phi$  for the standard dye quinine sulfate is 0.54, dissolved in 0.1 M  $\text{H}_2\text{SO}_4$  which has a refractive index ( $\eta$ ) of 1.33. The N1 sample was dissolved in water ( $\eta = 1.33$ ). All the fluorescence spectra were recorded at same excitation of 365 nm. By comparing the photoluminescence integrated areas (excited at 365 nm) and absorbance values (at 365 nm) of the compound N1 with the reference dye, the quantum yield of compound N1 was found to be 5.1% (0.051).

## Conflicts of interest

“There are no conflicts to declare”.



## Acknowledgements

This work was supported by the DST-INSPIRE Faculty Scheme, Department of Science and Technology, Govt. of India, (Award No. DST/INSPIRE/04/2018/000445). We gratefully acknowledged IASST for all the support provided while implementing the project. AcSIR is recognized with appreciation for providing PhD guideship to A. K.

## Notes and references

- 1 S. L. Sonawane and S. K. Asha, *ACS Appl. Mater. Interfaces*, 2016, **8**, 10590.
- 2 Z. Chi, X. Zhang, B. Xu, X. Zhou, C. Ma, Y. Zhang, S. Liu and J. Xu, *Chem. Soc. Rev.*, 2012, **41**, 3878.
- 3 X. Zhang, H. Dong and W. Hu, *Adv. Mater.*, 2018, **30**, 1801048.
- 4 H. Shen, A. Abtahi, B. Lussem, B. W. Boudouris and J. Mei, *ACS Appl. Electron. Mater.*, 2021, **3**, 2434.
- 5 S. K. B. Mane, Y. Mu, Z. Yang, E. Ubba, N. Shaishta and Z. Chi, *J. Mater. Chem. C*, 2019, **7**, 3522.
- 6 A. D. Pagar, M. D. Patil, D. T. Flood, T. H. Yoo, P. E. Dawson and H. Yun, *Chem. Rev.*, 2021, **121**, 6173.
- 7 J. Zhang, B. He, Y. Hu, P. Alam, H. Zhang, J. W. Y. Lam and B. Z. Tang, *Adv. Mater.*, 2021, **33**, 2008071.
- 8 X. Yan, F. Wang, B. Zheng and F. Huang, *Chem. Soc. Rev.*, 2012, **41**, 6042.
- 9 X. Ma and H. Tian, *Acc. Chem. Res.*, 2014, **47**, 1971.
- 10 J. Hu and S. Liu, *Acc. Chem. Res.*, 2014, **47**, 2084.
- 11 B. Yue and L. Zhu, *Chem.-Asian J.*, 2019, **14**, 2172.
- 12 W. L. Gong, M. P. Aldred, G.-F. Zhang, C. Li and M.-Q. Zhu, *J. Mater. Chem. C*, 2013, **1**, 7519.
- 13 W. Lin, Q. Tan, H. Liang, K. Y. Zhang, S. Liu, R. Jiang, R. Hu, W. Xu, Q. Zhao and W. Huang, *J. Mater. Chem. C*, 2015, **3**, 1883.
- 14 L. J. Chen and H. B. Yang, *Acc. Chem. Res.*, 2018, **51**, 2699.
- 15 N. Zhou, R. Hailes, Y. Zhang, Z. Chen, I. Manners and X. He, *Polym. Chem.*, 2020, **11**, 2700.
- 16 C. Demangeat, Y. Dou, B. Hu, Y. Bretonnière, C. Andraud, A. D'Aléo, J. W. Wu, E. Kim, T. L. Bahers and A. J. Attias, *Angew. Chem., Int. Ed.*, 2021, **133**, 2476.
- 17 A. Mukherjee, T. Sakurai, S. Seki and S. Ghosh, *Langmuir*, 2020, **36**, 13096.
- 18 J. D. Tovar, *Acc. Chem. Res.*, 2013, **46**, 1527.
- 19 T. Panda, D. K. Maiti and M. K. Panda, *ACS Appl. Mater. Interfaces*, 2018, **10**, 29100.
- 20 S. S. Babu, K. K. Kartha and A. Ajayaghosh, *J. Phys. Chem. Lett.*, 2010, **1**, 3413.
- 21 F. S. Kim, G. Ren and S. A. Jenekhe, *Chem. Mater.*, 2011, **23**, 682.
- 22 L. Maggini and D. Bonifazi, *Chem. Soc. Rev.*, 2012, **41**, 211.
- 23 M. A. Kobaisi, S. V. Bhosale, K. Latham, A. M. Raynor and S. V. Bhosale, *Chem. Rev.*, 2016, **116**, 11685.
- 24 A. WeiBenstein, V. Grande, C. R. S. Möllera and F. Würthner, *Org. Chem. Front.*, 2018, **5**, 2641.
- 25 P. Choudhury, S. Sarkar and P. K. Das, *Langmuir*, 2018, **34**, 14328.
- 26 S. K. Keshri, K. Mandal, Y. Kumar, D. Yadav and P. Mukhopadhyay, *Chem.-Eur. J.*, 2021, **27**, 1.
- 27 N. B. Kolhe, R. N. Devi, S. P. Senanayak, B. Jancy, K. S. Narayan and S. K. Asha, *J. Mater. Chem.*, 2012, **22**, 15235–15246.
- 28 A. Sikder and S. Ghosh, *Mater. Chem. Front.*, 2019, **3**, 2602–2616.
- 29 (a) A. P. Malvino and J. A. Brown, *Digital computer electronics*, McGraw-Hill, Glencoe, 1992; (b) R. J. Mitchell, *Microprocessor Systems: An Introduction*, Palgrave Macmillan, 1995.
- 30 M. E. S. West, C.-Y. Yao, G. Melaugh, K. Kawamoto, S. Uchiyama and A. P. de Silva, *Chem.-Eur. J.*, 2021, **27**, 1.
- 31 E. T. Ecik, A. Atilgan, R. Guliyev, T. B. Uyar, A. Gumus and E. U. Akkaya, *Dalton Trans.*, 2014, **43**, 67.
- 32 T. A. Molden, M. C. Grillo and D. M. Kolphashchikov, *Chem.-Eur. J.*, 2021, **27**, 2421.
- 33 A. Mondal, A. R. Chowdhury, S. Bhuyan, S. K. Mukhopadhyay and P. Banerjee, *Dalton Trans.*, 2019, **48**, 4375.
- 34 H. Swaminathan and K. Balasubramanian, *J. Appl. Phys.*, 2019, **126**, 084503.
- 35 M. R. Ajayakumar, G. Hundal and P. Mukhopadhyay, *Chem. Commun.*, 2013, **49**, 7684.
- 36 G. T. Selvan, C. Varadaraju, R. T. Selvan, I. V. M. V. Enoch and P. M. Selvakumar, *ACS Omega*, 2018, **3**, 7985.
- 37 D. Singharoy, S. Chowdhury, S. S. Mati, S. Ghosh, K. Chattopadhyay and S. C. Bhattacharya, *Chem.-Eur. J.*, 2017, **23**, 16516.
- 38 S. Yang, J. Liu, Z. Cao, M. Li, Q. Luo and D. Qu, *Dyes Pigm.*, 2018, **148**, 341.
- 39 H. J. Bora, P. Barman, N. S. Sarma and A. Kalita, *ACS Appl. Electron. Mater.*, 2021, **3**, 2720.
- 40 D. Zhou, Y. Wang, J. Jia, W. Yu, B. Qu, X. Li and X. Sun, *Chem. Commun.*, 2015, **51**, 10656.
- 41 F. Han, L. Chi, W. Wu, X. Liang, M. Fu and J. Zhao, *J. Photochem. Photobiol., A*, 2008, **196**, 10.
- 42 S. Yang, J. Liu, P. Zhou and G. He, *J. Phys. Chem. B*, 2011, **115**, 10692.
- 43 S. Uchiyama, K. Takehira, T. Yoshihara, S. Tobita and T. Ohwada, *Org. Lett.*, 2006, **8**, 5869.
- 44 E. C. Lim, *J. Phys. Chem.*, 1986, **90**, 6770–6777.
- 45 J. S. de Melo, R. S. Becker, F. Elisei and A. L. Maçanita, *J. Phys. Chem.*, 1997, **107**, 6062.
- 46 A. Kobayashi, K. Takehira, T. Yoshihara, S. Uchiyama and S. Tobita, *Photochem. Photobiol. Sci.*, 2012, **11**, 1368.
- 47 S. Basak, N. Nandi, S. Paul and A. Banerjee, *ACS Omega*, 2018, **3**, 2174.
- 48 B. Garai, A. Mallick and R. Banerjee, *Chem. Sci.*, 2016, **7**, 2195.
- 49 N. Dhenadhayalan and K. C. Lin, *Sci. Rep.*, 2015, **5**, 10012.
- 50 R. Dalapati and S. Biswas, *Chem.-Asian J.*, 2019, **16**, 2822.
- 51 Z. Deller, L. A. Jones and S. Maniam, *Green Chem.*, 2021, **23**, 4955.
- 52 M. S. Sánchez, N. Getachew, K. Díaz, M. D. García, Y. Chebudeb and I. Díaz, *Green Chem.*, 2015, **17**, 1500.
- 53 B. Chowdhury, S. Sinha, R. Dutta, S. Mondal, S. Karmakar and P. Ghosh, *Inorg. Chem.*, 2020, **59**, 13371.

